# Astigmatism-corrected Czerny–Turner imaging spectrometer for broadband spectral simultaneity

Qingsheng Xue

Changchun Institute of Optics, Fine Mechanics and Physics, Chinese Academy of Sciences, Changchun, Jilin 130033, China (qshxue2006@163.com)

Received 1 December 2010; revised 21 January 2011; accepted 28 January 2011; posted 28 January 2011 (Doc. ID 139042); published 24 March 2011

A low-cost, broadband, astigmatism-corrected Czerny–Turner arrangement with a fixed plane grating is proposed. A wedge cylindrical lens is used to correct astigmatism over a broadband spectral range. The principle and method of astigmatism correction are described in detail. We compare the performance of this modified Czerny–Turner arrangement with that of the traditional Czerny–Turner arrangement by using a practical Czerny–Turner imaging spectrometer example. © 2011 Optical Society of America

*OCIS codes:* 300.0300, 300.6190, 120.4570, 120.0120, 120.0280.

## 1. Introduction

The Czerny–Turner spectrometer with a rotary grating and a one-dimensional detector is a commonly used instrument for resolving the spectral intensity of radiation. Several applications in frequency-domain optical coherence tomography [1,2], atmospheric sounding [3], and spatially resolved ultrashort pulse measurement [4] require high-quality imaging over a broadband spectral simultaneity. However, the traditional Czerny–Turner design, using two spherical mirrors and a plane grating, suffers from astigmatism due to the different focal lengths in the tangential and sagittal planes resulting from the off-axis incidence to spherical mirrors. The astigmatism can be ignored in one-dimensional spectroscopy by locating an exit slit at the tangential focal plane. However, the uncorrected astigmatism does result in degraded performance in some applications using a fixed grating and a two-dimensional detector. Some methods to reduce or remove the limiting astigmatism have been investigated, such as using an additional convex mirror [5], using a cylindrical grating [6], compensating optics before the entrance slit [7], using toroidal mirrors [8], or using free-form mirrors [9]. Indeed, there have been several recent developments featuring broadband astigmatism correction without using nonspherical mirrors or nonplanar gratings. These recent designs include placing a glass plate before the entrance slit [10], using divergent illumination [11], and tilting a cylindrical lens [12]. However, the method of placing a glass plate before the entrance slit required the length of the glass piece to be fairly precise, and the light intensity lost with this method was very serious, approximately 12%. When using divergent illumination, the grating that was under divergent illumination not only induced astigmatism, but also induced coma, and the induced coma also influenced the imaging quality. When using the tilting cylindrical lens, astigmatism cannot be corrected sufficiently when the slit height is larger than 5 mm, which is necessary in some applications (for example, spaceborne limb atmospherical sounding). Here we propose a low-cost method that uses a wedge cylindrical lens to correct the astigmatism over broadband spectral simultaneity. By using this method, astigmatism can be corrected sufficiently when the slit height is larger than 5 mm. The wedge cylindrical lens positioned between the spherical focusing mirror and the detector is a low-cost optical component. In Section 2, we present how a wedge cylindrical lens can correct the astigmatism over broadband spectral simultaneity. In Section 3, we program a design procedure, calculating the initial structural parameters. In Section 4, we present a ray-tracing analysis of

0003-6935/11/101338-07$15.00/0

such a design and compare the novel method of using the wedge cylindrical lens with previous work, specifically with a divergent illumination method and a tilting cylindrical lens method. A summary is given in Section 5.

## 2. Broadband Astigmatism Correction

For a mirror of radius $r$ that images an object lying at a distance $l$ from the mirror vertex, there are two image distances: the sagittal astigmatic image distance ($l'_s$) and the tangential astigmatic image distance ($l'_t$). If the chief ray makes an angle $\alpha/2$ with the mirror radius, the imaging relations can be written as

$$\frac{1}{l'_s}-\frac{1}{l}=\frac{2\cos(\alpha/2)}{r}, \tag{1}$$

$$\frac{1}{l'_t}-\frac{1}{l}=\frac{2}{r\cos(\alpha/2)}. \tag{2}$$

$l'_s$ and $l'_t$ are measured along the chief ray. In the collimating light, $l=\infty$. Therefore, the sagittal focal length ($f'_s$) and tangential focal length ($f'_t$) become

$$f'_s=r/2\cos(\alpha/2), \tag{3}$$

$$f'_t=(r/2)\cos(\alpha/2). \tag{4}$$

The difference in astigmatic foci yielded by the two off-axis spherical mirrors of Czerny–Turner can be derived as [13]

$$\delta f'=(r_1/2)[\sin(\alpha_1/2)\tan(\alpha_1/2)]+(r_2/2)[\sin(\alpha_2/2)\tan(\alpha_2/2)], \tag{5}$$

where $r_1$ is the radius of the first spherical mirror (collimating mirror), $r_2$ is the radius of the second spherical mirror (focusing mirror), $\alpha_1/2$ is the off-axis incident angle on the first mirror, and $\alpha_2/2$ is the off-axis incident angle on the second mirror. When the off-axis incident angle $\alpha_1/2$ and $\alpha_2/2$ are not large, Eq. (5) is valid. In our modified design, a wedge cylindrical lens is located between the second spherical mirror and detector, as shown in Fig. 1, which displays in (a) the tangential view and in (b) the sagittal view. As illustrated in Fig. 1(a), the change of tangential focus introduced by the wedge cylindrical lens (i.e., optical wedge in the tangential view) is given by

$$l'_{wt}-l_{wt}=[(n-1)/n]\cdot t, \tag{6}$$

where the subscript $w$ stands for wedge, $l_{wt}$ is the tangential object distance, $l'_{wt}$ is the tangential imaging distance, $n$ is the refractive index, and $t$ is the central thickness of the wedge cylindrical lens. In the sagittal view, the imaging formula of the wedge cylindrical lens is

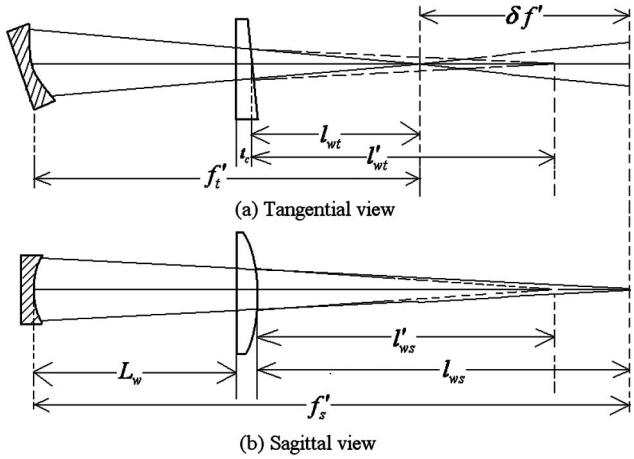


Fig. 1. Astigmatism correction by a wedge cylindrical lens in (a) tangential view and (b) sagittal view before the detector. The solid rays denote the rays not using a wedge cylindrical lens, and the dashed rays denote the rays using a wedge cylindrical lens.

$$1/l'_{ws}-1/l'_{wt}=1/f'_{ws}, \tag{7}$$

where $l_{ws}$ is the sagittal objective distance, $l'_{ws}$ is the sagittal image distance, and $f'_{ws}$ is the focal length of wedge cylindrical lens.

As illustrated in Fig. 1, when

$$\delta f'=l'_{wt}-l_{wt}+l_{ws}-l'_{ws}, \tag{8}$$

the astigmatism is corrected. Substituting Eqs. (6) and (7) into Eq. (8) yields

$$\delta f'=[(n-1)/n]t+l^2_{ws}/(f'_{ws}+l_{ws}). \tag{9}$$

The incident angles to the second spherical mirror are different for different wavelengths because of different diffractive directions at the grating, as shown in Fig. 2. The variation in $\alpha_2/2$ across the second mirror results in a variation in astigmatism $\delta f'$ across the detector. $H$ is the distance between the chief ray of the central wavelength with the chief ray of other wavelengths in the tangential view. The varying

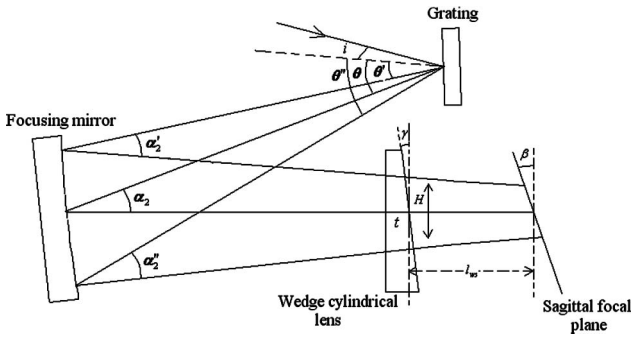


Fig. 2. Astigmatism correction by a wedge cylindrical lens for broadband spectral simultaneity in the tangential view of the chief ray tracing for the different wavelengths; $i$ is the angle incident to the grating and $H$ is the distance between the chief ray of the central wavelength with the chief ray of other wavelengths in the tangential view.

astigmatism can be simultaneously corrected by a wedge cylindrical lens with an optimized wedge angle.

By differentiating Eq. (9) with respect to $\lambda$, we obtain

$$\frac{\mathrm{d}(\delta f')}{\mathrm{d}(\alpha_2/2)}\cdot\frac{\mathrm{d}(\alpha_2/2)}{\mathrm{d}\theta}\cdot\frac{\mathrm{d}\theta}{\mathrm{d}\lambda}=\frac{t}{n^2}\cdot\frac{\mathrm{d}n}{\mathrm{d}\lambda}+\frac{n-1}{n}\cdot\frac{\mathrm{d}t}{\mathrm{d}\lambda}-\frac{2f'_{ws}l_{ws}+l_{ws}^2}{(f'_{ws}+l_{ws})^2}\cdot\frac{\mathrm{d}l_{ws}}{\mathrm{d}H}\cdot\frac{\mathrm{d}H}{\mathrm{d}\lambda}. \tag{10}$$

The differentiation $\mathrm{d}t/\mathrm{d}\lambda$ is calculated as

$$\frac{\mathrm{d}t}{\mathrm{d}\lambda}=\frac{\mathrm{d}t}{\mathrm{d}H}\cdot\frac{\mathrm{d}H}{\mathrm{d}\lambda}. \tag{11}$$

The differentiation $\mathrm{d}t/\mathrm{d}H$ is derived from geometry as

$$\left.\frac{\mathrm{d}t}{\mathrm{d}H}\right|_{H=0}=\tan\gamma, \tag{12}$$

where $\gamma$ is the wedge angle of the wedge cylindrical lens, as shown in Fig. 2. The differentiation $\mathrm{d}H/\mathrm{d}\lambda$ is the linear dispersion of the grating with the focusing mirror $r_2$ at the central wavelength, which is given as

$$\left.\frac{\mathrm{d}H}{\mathrm{d}\lambda}\right|_{\lambda=\lambda_c}=\frac{r_2}{2d\cos\theta}, \tag{13}$$

where $\lambda_c$ is the central wavelength and $d$ is the groove spacing of the grating. The differentiation $\mathrm{d}l_{ws}/\mathrm{d}H$ is derived from geometry as

$$\left.\frac{\mathrm{d}l_{ws}}{\mathrm{d}H}\right|_{H=0}=\tan(\beta-\gamma), \tag{14}$$

where $\beta$ is the tilt angle of the focal plane with respect to the chief ray, as shown in Fig. 2. We have found that, when

$$L_{gf}=r_2\cos(\alpha_2/2), \tag{15}$$

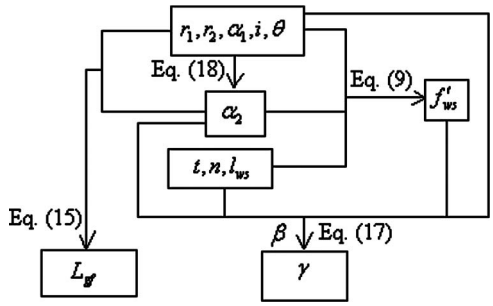


Fig. 3. Program block diagram for calculating the initial structural parameters.

**Table 1. Imaging Spectrometer Basic Parameters**

| Parameter | Value |
|---|---|
| Central wavelength (nm) | 500 |
| $r_1$ (mm) | 402.5 |
| $r_2$ (mm) | 427.06 |
| $\alpha_1/2$ (°) | 8 |
| $\alpha_2/2$ (°) | 9.133 |
| $d$ ($\mu$m) | 3.33 |
| $i$ (°) | 5 |
| $\theta$ (°) | 13.719 |
| $n$ | 1.462 |
| $t$ | 5 |
| $\beta$ (°) | 7.86 |
| $l_{ws}$ (mm) | 26.54 |

the incident angles to the second spherical mirror (focusing mirror) for different wavelengths are approximately identical [14], i.e.,

$$\frac{\mathrm{d}(\alpha_2/2)}{\mathrm{d}\theta}=0, \tag{16}$$

where $L_{gf}$ is the distance between the grating and the focusing mirror. Substituting Eqs. (11)–(14) and (16) into Eq. (10) gives

$$\frac{t}{n^2}\left(\frac{\mathrm{d}n}{\mathrm{d}\lambda}\right)_{\lambda=\lambda_c}+\left(\frac{n-1}{n}\right)\tan\gamma-\frac{2f'_{ws}l_{ws}+l_{ws}^2}{(f'_{ws}+l_{ws})^2}\tan(\beta-\gamma)=0, \tag{17}$$

and the wedge angle $\gamma$ can be solved from Eq. (17).

## 3. Design Procedure

The results of Section 2 lead to the following design procedure. We first choose the mirror anglea $\alpha_1$ and $\alpha_2$ and the mirror radii $r_1$ and $r_2$ based on the coma-corrected condition that is known as the Shafer equation [15]:

$$\frac{\sin(\alpha_1/2)}{\sin(\alpha_2/2)}=\left(\frac{r_1}{r_2}\right)^2\left(\frac{\cos\theta}{\cos i}\right)^3. \tag{18}$$

We then choose the central thickness $t$, the refractive index $n$, and the sagittal objective distance $l_{ws}$, and derive the sagittal focal length of the wedge cylindrical lens $f'_{ws}$ from Eq. (9). We derive the distance $L_{gf}$ from Eq. (15). Finally, we choose the tilt angle of detector $\beta$ and derive the wedge angle $\gamma$ from Eq. (17). Thus, all the structural parameters can be obtained. We programmed the procedure calculating the initial parameters, written in MATLAB. The program block diagram is shown in Fig. 3.

**Table 2. Imaging Spectrometer Designed Parameters**

| Parameter | Calculated | Ray-Tracing Optimized |
|---|---|---|
| $L_{gf}$ (mm) | 421.65 | 307.64 |
| $f'_{ws}$ (mm) | 25.5 | 24.14 |
| $\gamma$ (°) | 4.5 | 5.089 |

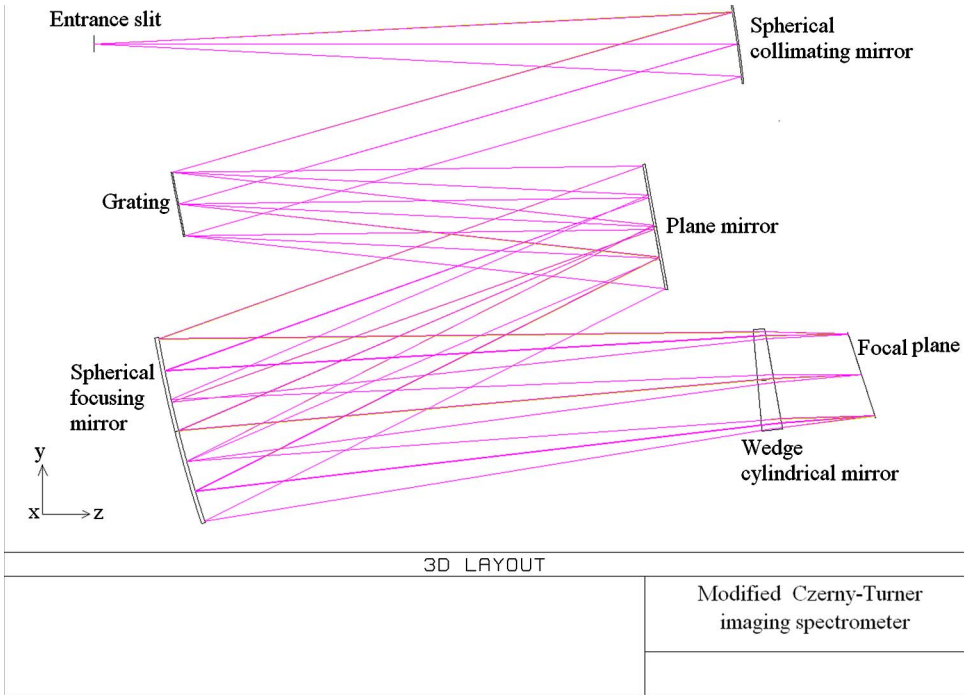


Fig. 4. (Color online) Layout of the modified Czerny–Turner imaging spectrometer.

## 4. Ray-Tracing Analysis

In this section, we present a design example to illustrate the application of the modified arrangement. We calculate initial structural parameters using the program presented above, and then model and analyze this system using the optical system design program ZEMAX [16].

The imaging spectrometer is designed to sounding atmosphere composition in limb view geometry with a fixed plane grating (300 grooves/mm). The spectrometer is a UV-to-visible system with a broadband spectral range from 0.3 to 0.7 $\mu$m. The object numerical aperture is 0.05 and the slit size is 5.2 mm× 50 $\mu$m. A CCD with a size of 25.65 mm × 25.65 mm (pixel size is 25 $\mu$m × 25 $\mu$m, and pixel number is 1024 × 1024) is used. We select an off-the-shelf grating. The groove spacing $d$ is 3.33 $\mu$m, which corresponds to 300 grooves/mm. Fused silica is chosen as the material of the wedge cylindrical lens, and the refractive index $n$ is 1.62 at central wavelength 500 nm. The basic parameters of the spectrometer are shown in Table 1. From these, we calculated $L_{gf}$, $f'_{ws}$, and wedge angle $\gamma$ using the procedure in Sections 3, to give the values in Table 2. These are used as the initial parameters for an optimization using the ZEMAX program. The optimized parameters are shown in Table 2.

The focal of the wedge cylindrical lens was calculated to be 25.5 mm using Eqs. (5) and (9), which is in close agreement with the optimized value of 24.14 mm. The wedge angle $\gamma$ of the wedge cylindrical

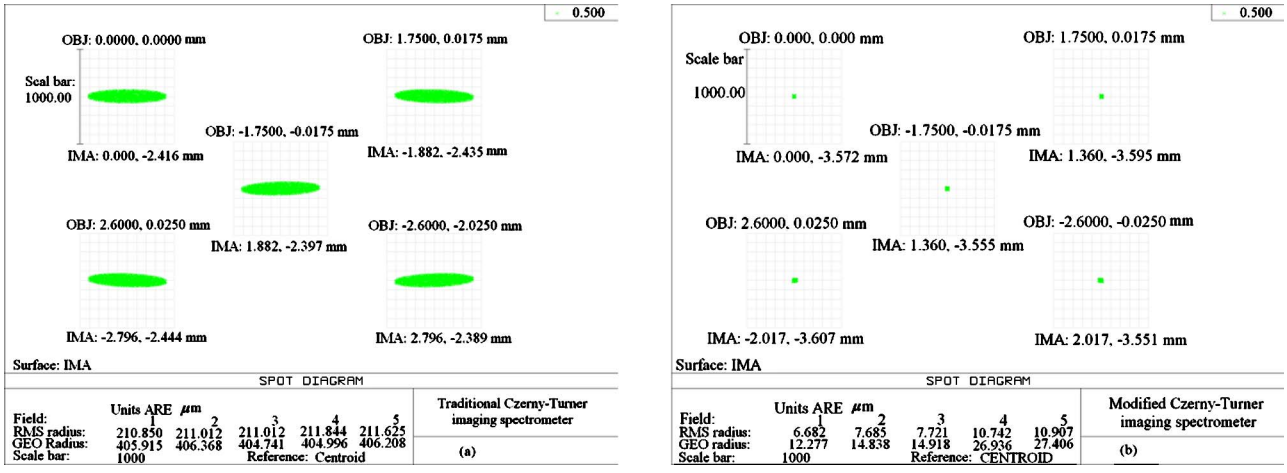


Fig. 5. (Color online) Spot diagrams of different fields of view for (a) a traditional Czerny–Turner spectrometer and (b) the modified Czerny–Turner imaging spectrometer.

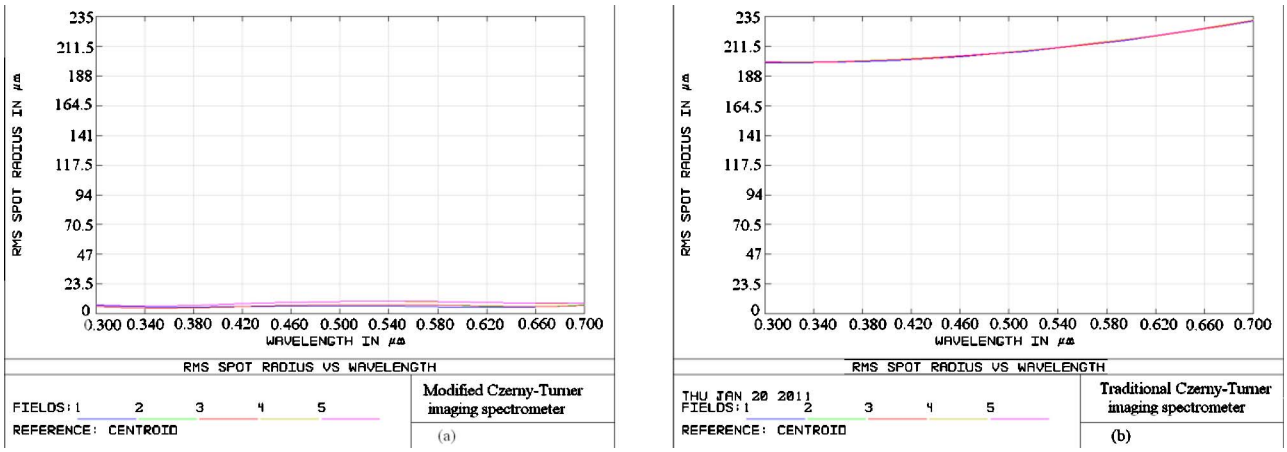


Fig. 6. (Color online) RMS spot radius versus wavelength for (a) the modified Czerny–Turner imaging spectrometer and (b) a traditional Czerny–Turner spectrometer.

lens was calculated to be 4.5° using Eq. (17), which is close to the optimized vale 5.089°. To diminish the geometrical scale of the spectrometer, we place a plane mirror between the grating and the spherical focusing mirror. The optimized layout is shown in Fig. 4.

With the help of ZEMAX, optical performances the system can be predicted and plotted. Spot diagrams at the detector surface are calculated for different fields of view at the entrance slit with our modified configuration and the traditional Czerny–Turner configuration. We shall first demonstrate

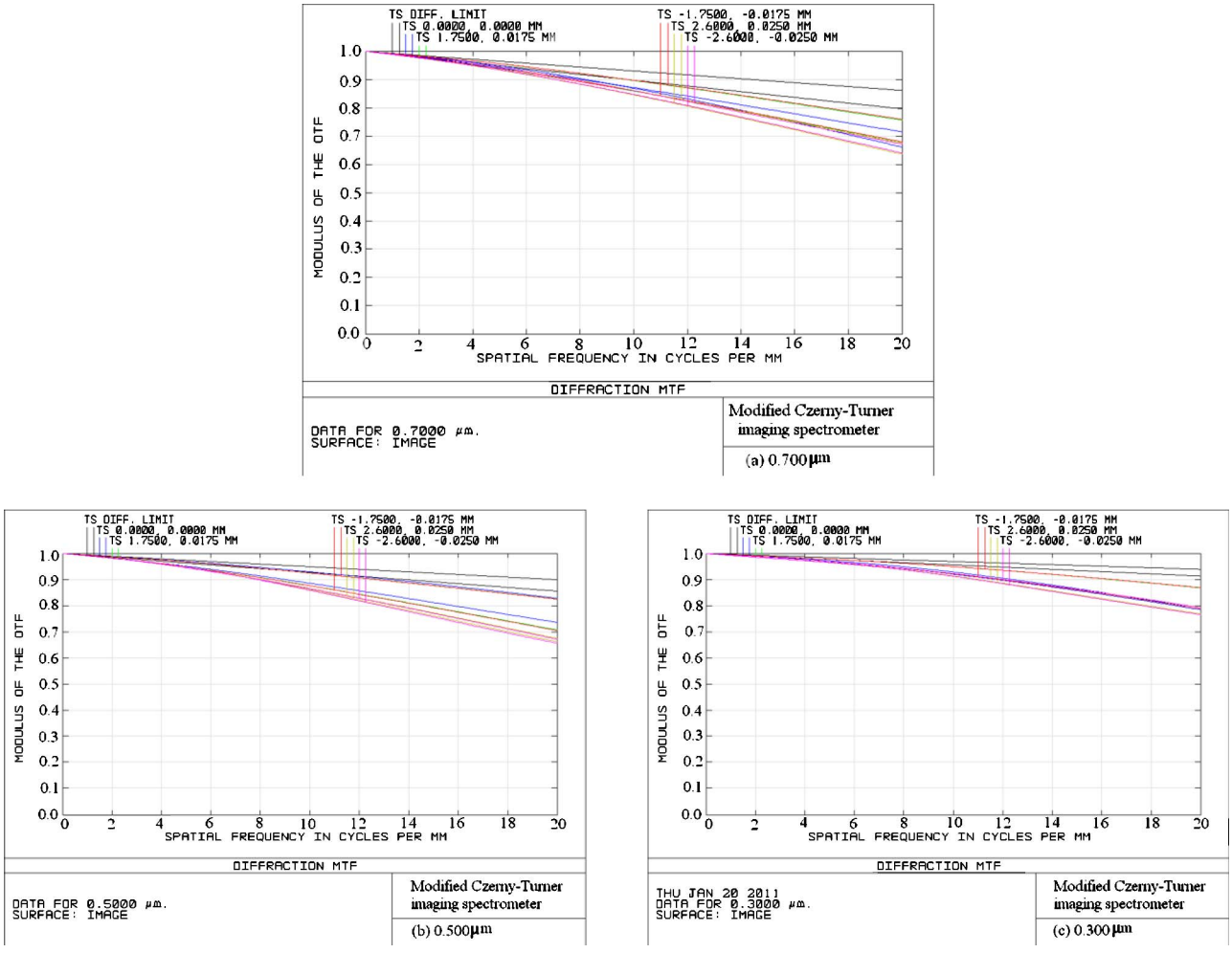


Fig. 7. (Color online) MTF of the modified Czerny–Turner imaging spectrometer at the central and marginal wavelengths.

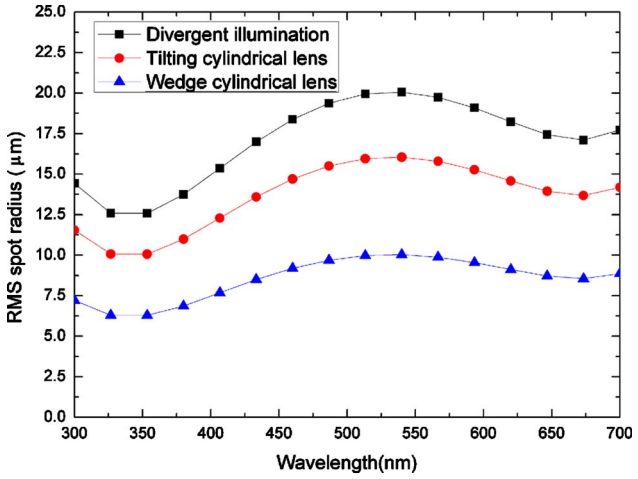


Fig. 8. (Color online) RMS spot radius versus wavelength for three different methods: the method reported here (blue triangles), a method using divergent illumination (black squares), and a method using a tilting cylindrical lens (red circles).

the expanded image that is due to the astigmatism in the traditional Czerny–Turner spectrometer when not using a wedge cylindrical lens. In fact, the expand image of approximately 20 $\mu$m (tangential) × 1 mm (sagittal) is obtained as shown in Fig. 5(a). We then show the result of astigmatism correction in our modified Czerny–Turner imaging spectrometer using a wedge cylindrical lens. We obtain substantially improved images with a spot size of approximately 20 $\mu$m, which is less than 1/50 in the sagittal direction when compared with those obtained without using a wedge cylindrical lens, as shown in Fig. 5(b).

To show the result of astigmatism correction for broadband spectral simultaneity, the RMS spot radius is given as a function of wavelength for the modified Czerny–Turner imaging spectrometer (using the wedge cylindrical lens) and the traditional Czerny–Turner spectrometer (not using wedge cylindrical lens). Obviously, when the wedge cylindrical lens is used, the RMS spot radius is less than 10 $\mu$m over the broad working wavelength band from 300 to 700 nm, as shown in Fig. 6(a). The results demonstrate that astigmatism is simultaneously corrected over a broad spectral range. However, when the cylindrical lens is not used, the RMS spot radius is larger than 200 $\mu$m, resulting from the devastating astigmatism, as shown in Fig. 6(b). The modulation transfer function (MTF) curves are given as a function of spatial frequency in Figs. 7(a)–7(c). It is clear that the MTF of each field is larger than 0.64 at the CCD's Nyquist frequency (20 line pairs/mm) for the central and marginal wavelengths. The results demonstrate that good imaging quality is simultaneously obtained over the broad wavelength region and satisfies the application requirement.

To see how much the performance is improved, we compared the new design with recent astigmatism-correction methods, specifically with the divergent illumination method and a tilting cylindrical lens method, respectively, in the same field of view (FOV) and numerical aperture condition and using the same detector size (i.e., FOV $x = 2.6$ mm, $y = 0.025$ mm, NA $= 0.05$, pixel size 25 $\mu$m, pixel number $1024 \times 1024$) and grating dispersion. The RMS spot radius versus wavelength is shown in Fig. 8. As seen in Fig. 8, the RMS spot radius is approximately less than 10 $\mu$m using our novel method than that using the divergent illumination method, and approximately less than 6 $\mu$m using our novel method than that using a tilting cylindrical lens method. The results demonstrate that the new method reported here is more valid than the recently published methods.

## 5. Summary

We have designed a Czerny–Turner imaging spectrometer using a wedge cylindrical lens to correct astigmatism for broadband spectral simultaneity. The traditional Czerny–Turner spectrometer, while configured to correct coma, suffers from astigmatism due to the tilt of the spherical mirrors. There have been a number of attempts to overcome this limitation, including the use of free-form mirrors and cylindrical gratings. Our design supports the use of a wedge cylindrical lens, which is less expensive than free-form mirrors or cylindrical gratings. This design will be useful for atmospheric sounding, as well as having broad application in astronomical imaging and studying the structure of ultrashort pulses.

The work described in this paper is supported by the National Natural Science Foundation of China (NSFC) under grant 40675083.

## References and Notes

1. J. P. Rolland, P. Meemon, S. Murali, K. P. Thompson, and K. S. Lee, "Gabor-based fusion technique for optical coherence microscopy," Opt. Express **18**, 3632–3642 (2010).
2. S. Murali, P. Meemon, K. S. Lee, W. P. Kuhn, K. P. Thompson, and J. P. Rolland, "Assessment of a liquid lens enabled *in vivo* optical coherence microscope," Appl. Opt. **49**, D145–D156 (2010).
3. R. D. McPeters, S. J. Janz, E. Hilsenrath, T. L. Brown, D. E. Flittner, and D. F. Heath, "The retrieval of $O_3$ profiles from limb scatter measurements: results from the Shuttle ozone limb sounding experiment," Geophys. Res. Lett. **27**, 2597–2600 (2000).
4. A. Wyatt, I. Walmsley, G. Stibenz, and G. Steinmeyer, "Sub-10 fs pulse characterization using spatially encoded arrangement for spectral phase interferometry for direct electric field reconstruction," Opt. Lett. **31**, 1914–1916 (2006).
5. G. R. Rosendahl, "Contributions to the optics of mirror systems and gratings with oblique incidence. III. Some applications," J. Opt. Soc. Am. **52**, 412–415 (1962).
6. M. L. Dalton, Jr., "Astigmatism compensation in the Czerny–Turner spectrometer," Appl. Opt. **5**, 1121–1123 (1966).
7. M. Goto and S. Morita, "Spatial distribution measurement of atomic radiation with an astigmatism-corrected Czerny–Turner-type spectrometer in the Large Helical Device," Rev. Sci. Instrum. **77**, 10F124 (2006).
8. Q. Xue, S. Wang, and F. Li, "Czerny-Turner imaging spectrometer for broadband spectral simultaneity," Chin. Opt. Lett. **7**, 861–864 (2009).

9. L. Xu, K. Chen, Q. He, and G. Jin, "Design of freeform mirrors in Czerny–Turner spectrometers to suppress astigmatism," Appl. Opt. **48**, 2871–2879 (2009).
10. C. Chrystal, K. H. Burrell, and N. A. Pablant, "Straightforward correction for the astigmatism of a Czerny–Turner spectrometer," Rev. Sci. Instrum. **81**, 023503 (2010).
11. D. R. Austin, T. Witting, and I. A. Walmsley, "Broadband astigmatism-free Czerny–Turner imaging spectrometer using spherical mirrors," Appl. Opt. **48**, 3846–3853 (2009).
12. K. S. Lee, K. P. Thompson, and J. P. Rolland, "Broadband astigmatism-corrected Czerny–Turner spectrometer," Opt. Express **18**, 23378–23384 (2010).
13. M. L. Dalton Jr., "Astigmatism compensation in the Czerny–Turner spectrometer," Appl. Opt. **5**, 1121–1123 (1966).
14. Q. Xue, S. Wang, and F. Lu, "Aberration-corrected Czerny–Turner imaging spectrometer with a wide spectral region," Appl. Opt. **48**, 11–16 (2009).
15. A. B. Shafer, "Correcting for astigmatism in the Czerny–Turner spectrometer and spectrograph," Appl. Opt. **6**, 159–160 (1967).
16. ZEMAX is a trademark of Zemax Development Corporation, Bellevue, Washington 98004, USA.